Journal of Ginseng Research 48 (2024) 417–424

Contents lists available at ScienceDirect

Journal of Ginseng Research

journal homepage: www.sciencedirect.com/journal/journal-of-ginseng-research

Research Article

Preparation and evaluation of proliposomes formulation for enhancing the oral bioavailability of ginsenosides

Duy-Thuc Nguyen [a], Min-Hwan Kim [a], Min-Jun Baek [a], Nae-Won Kang [a], Dae-Duk Kim [a,b,*]

[a] College of Pharmacy and Research Institute of Pharmaceutical Sciences, Seoul National University, Seoul, Republic of Korea
[b] Natural Products Research Institute, Seoul National University, Seoul, Republic of Korea

ARTICLE INFO

Keywords:
Bioavailability
Ginsenosides
Oral
Proliposomes
Rg3

ABSTRACT

Background: This research main objective was to evaluate a proliposomes (PLs) formulation for the enhancement of oral bioavailability of ginsenosides, using ginsenoside Rg3 (Rg3) as a marker.
Methods: A novel PLs formulation was prepared using a modified evaporation-on-matrix method. Soy phosphatidylcholine, Rg3-enriched extract, poloxamer 188 (Lutrol® F 68) and sorbitol were mixed and dissolved using a aqueous ethanolic solution, followed by the removal of ethanol and lyophilization. The characterization of Rg3-PLs formulations was performed by powder X-ray diffractometry (PXRD), transmission electron microscopy (TEM) and *in vitro* release. The enhancement of oral bioavailability was investigated and analyzed by non-compartmental parameters after oral administration of the formulations.
Results: PXRD of Rg3-PLs indicated that Rg3 was transformed from crystalline into its amorphous form during the preparation process. The Rg3-encapsulated liposomes with vesicular-shaped morphology were generated after the reconstitution by gentle hand-shaking in water; they had a mean diameter of approximately 350 nm, a negative zeta potential (−28.6 mV) and a high entrapment efficiency (97.3%). The results of the *in vitro* release study exhibited that significantly more amount of Rg3 was released from the PLs formulation in comparison with that from the suspension of Rg3-enriched extract (control group). The pharmacokinetic parameters after oral administration of PLs formulation in rats showed an approximately 11.8-fold increase in the bioavailability of Rg3, compared to that of the control group.
Conclusion: The developed PLs formulation could be a favorable delivery system to improve the oral bioavailability of ginsenosides, including Rg3.

1. Introduction

Ginsenosides are reported to be the main active ingredients of Korean ginseng (*Panax ginseng* Meyer), and they have diverse pharmacological applications, including the treatment of diabetes, hypertension, as well as anti-inflammation and anticancer activities [1]. Although the clinical application of ginseng has a long history, its clinical application has been limited probably due to the low aqueous solubility of ginsenosides, which in turn results in poor absorption and low oral bioavailability [2–4]. Thus, various strategies of modern pharmaceutical techniques have been investigated to overcome the low oral bioavailability of ginsenosides for their clinical applications. These include microemulsions, nanoparticles and liposomes, among which liposomes have been intensively studied as an oral drug delivery system [5–9]. It was reported that liposomes improved the permeability and solubility of poorly water-soluble drugs in the gastrointestinal tract, thereby increasing the oral bioavailability [10,11]. However, the physical instability of liposomes during storage has been a major drawback, due to aggregation, precipitation, fusion and decomposition of phospholipids [12].

Proliposomes (PLs) formulation is a solid dosage form during storage that is rapidly hydrated and converted into liposomal structure when dispersed with the addition of a small amount of water [13,14]. PLs could be preferred over other colloidal solution dosage forms (*e.g.*, conventional liposomal dispersion) in terms of storage stability, while they still exert the benefits of liposomes after oral administration, including enhanced dissolution and/or absorption [13,15,16]. Moreover, the preparation processes of PLs are simpler and more cost-effective in comparison with conventional liposomes [13]. Thus, PLs have been widely applied as an oral drug delivery system, ranging

* Corresponding author. College of Pharmacy and Research Institute of Pharmaceutical Sciences, Seoul National University, Seoul, 08826, Republic of Korea.
E-mail address: ddkim@snu.ac.kr (D.-D. Kim).

https://doi.org/10.1016/j.jgr.2024.03.004
Received 12 January 2023; Received in revised form 22 January 2024; Accepted 10 March 2024
Available online 21 March 2024

from small molecule active pharmaceutical ingredients (APIs) such as celecoxib, valsartan, curcumin, and glutathione, to macromolecules such as daptomycin, recombinant human insulin and cyclosporin A [5,13,15,17–21]. Moreover, extracts from natural products, including *Ginkgo biloba* extract and polyphenols from *Rosmarinus officinalis* L., were also encapsulated in PLs formulation to enhance the stability and/or oral absorption [22]. However, the application of PLs for oral bioavailability enhancement of ginsenosides has not been reported [3].

Previously, we reported a novel preparation method for celecoxib-loaded PLs formulation using a solid dispersion technique with a high lipid content of up to 20% (w/w) as phosphatidyl choline [13,14]. Enhanced oral bioavailability of celecoxib (approximately 1.7-fold in comparison with free drug) was observed in a pharmacokinetic study in rats, which indicated that PLs formulation developed in our laboratory could be further applied for poorly water-soluble compounds, including ginsenosides. Thus, the aim of this research was to prepare the PLs formulation with high lipid content for loading ginsenoside Rg3-enriched extract (Rg3 extract), and to evaluate the effect on enhancing oral bioavailability. Ginsenoside Rg3 was chosen as a representative compound for analysis. The Rg3 extract-loaded PLs (Rg3-PLs) formulation was prepared and physicochemical properties were characterized using powder X-ray diffractometry (PXRD), dynamic

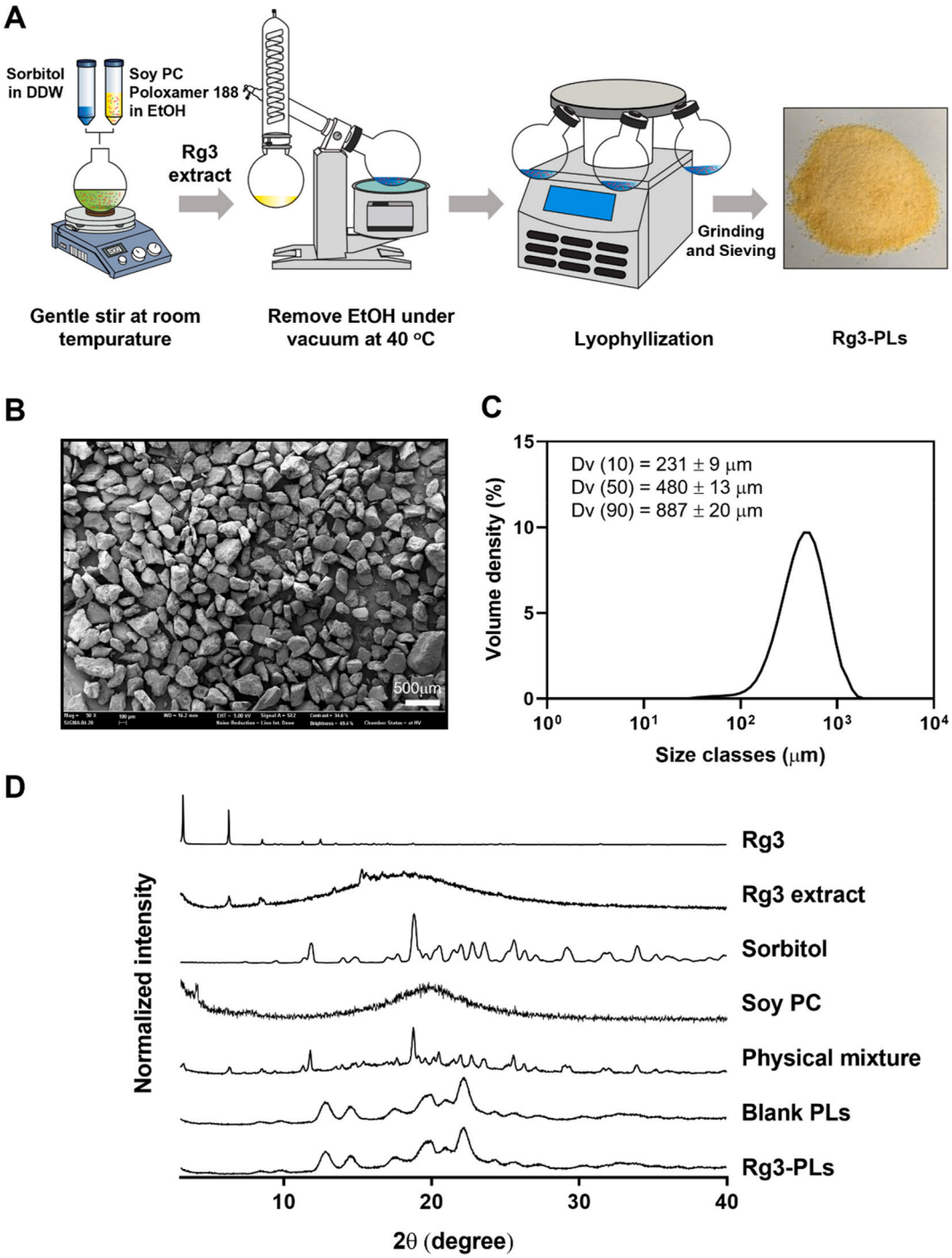

Fig. 1. (A) Schematic illustration of the Rg3-PLs preparation method. (B) FE-SEM image (the length of the scale bar is 500 μm) and (C) Particle size distribution of dried Rg3-PLs powder. (D) PXRD analysis of Rg3-PLs powder and excipients.

light scattering (DLS) and transmission electron microscopy (TEM) analysis. Pharmacokinetic study of Rg3 was conducted in rats after oral administration of Rg-3 PLs to confirm the enhancement of bioavailability.

2. Materials and methods

2.1. Materials

20(S)-Gingsenoside Rg3 (≥ 98%), sodium dodecylsulfate (SDS) and sorbitol were purchased from Sigma–Aldrich (St. Louis, MO, USA). Rg3 extract powder and soy phosphatidylcholine (SPC, 95%) were kindly gifted by KT&G Co. (Daejeon, South Korea) and Phytos (Gyeonggi, South Korea), respectively. Poloxamer 188 (Lutrol® F 68) was provided from BASF (Ludwigshafen, Germany). Ethanol was purchased from Daejung (Siheung-si, Gyeonggi, South Korea) and dimethyl sulfoxide (DMSO) was from Duksan (Gyeonggi-do, South Korea). Fetal bovine serum (FBS), streptomycin, penicilin and DMEM (Dulbecco's modified Eagle medium) for cell culture were purchased from Welgene (Gyeongsangbuk-do, South Korea). The purity of other reagents was analytical grade or higher.

2.2. Preparation of ginsenoside Rg3-enriched extract-loaded proliposomes (Rg3-PLs)

The solvent evaporation-on-matrix method that we previously reported was applied to prepare Rg3-PLs with slight modification (Fig. 1A) [13,16]. Briefly, SPC (800 mg) was completely dissolved in ethanol (8.75 mL), followed by adding poloxamer 188 (40 mg) to create a clear yellowish solution. Separately, sorbitol (3160 mg) was dissolved in 3.75 mL of double-deionized water (DDW). In a round-bottom flask, these two solutions were thoroughly stirred and mixed. Under gentle stirring at 100 rpm, 250 mg of Rg3 extract was slowly added for 30 min until all components were dissolved. The mixture was then placed *in vacuo* for 10 min at 40 °C to remove ethanol using a rotary evaporator, followed by the immediate lyophilization for 24 h. Finally, Rg3-PLs powder was obtained by grinding (using a mortar and pestle) and sieving. The powder fraction between the sieve No. 25 and 100 (US standard) was collected. The pale yellowish Rg3-PLs powder was put at −20 °C for storage and further experiments. The blank PLs for control experiments were prepared following the same procedure except the addition of Rg3 extract.

2.3. Physicochemical characterization of Rg3-PLs

2.3.1. Rg3 content and powder X-ray diffractometry of Rg3-PLs powder

The content of Rg3 in Rg3-PLs powder was analyzed by a liquid chromatography-tandem electrospray ionization mass spectrometry (HPLC−MS/MS, Agilent, CA, USA). Briefly, 10 mg of Rg3-PLs powder was completely dissolved in 1 mL of the cosolvent of DDW and ACN (1:1, v/v). Then, it was properly diluted with methanol for LC−MS/MS analysis, where a 50 μL aliquot was added with 250 μL of acetonitrile containing valsartan (100 ng/mL) as an internal standard. The mobile phase consisted of 0.1% (v/v) formic acid aqueous solution (solvent A) and 0.1% (v/v) formic acid in ACN (solvent B). The mobile phase was run at a constant flow rate of 0.4 mL/min in a gradient mode as the following A to B ratio: constant at 60:40 for 0–11 min, changed from 60:40 to 5:95 ratio for 11–15 min, returned to 60:40 ratio for 15–20 min and kept unchanged for 20–25 min. The injection volume of the sample was 5 μL, the column for separation was a C_{18} reversed-phase column (BDS Hypersil C_{18} 100 × 2.1 mm, 2.4 μm, Thermo Scientific, Waltham, MA, USA) at 40 °C. The *m/z* (mass-to-charge) ratio of the precursor and product ions, collision energy and fragmentor voltage were 783.6, 459.5, 50 eV, and 320 V for Rg3 and 434.1, 350.0, 18 eV and 140 V for valsartan, respectively. Rg3 and valsartan were eluted at 10.8 min and 2.2 min, respectively. At the lower limit of quantification (LLOQ) of 2 ng/mL, the signal-to-noise (S/N) ratio of the Rg3 peak was higher than 5.5. The linear calibration curve of the Rg3 standard solution showed a correlation coefficient (R^2) of 0.99 in the range of 2–2000 ng/mL. The Rg3 content (%) in Rg3-PLs was calculated by the following equation:

$$\text{Rg3 content } (\%) = \frac{X}{X_0} \times 100$$

where, X_0 is the initial amount of Rg3-PLs powder (mg) and X is the amount of Rg3 determined by LC−MS/MS analysis (mg).

Powder X-ray diffractometry (PXRD) analysis of Rg3-PLs in the solid-state was conducted to evaluate the change in crystalline of Rg3 and the excipients in the Rg3-PLs during the preparation process. The samples were analyzed using a D8 Advance with DAVINCI, Bruker Inc., (Karlsruhe, Germany), which was equipped with CuKα1 radiation at 1.5418 Å. The tube current was 40 mA and the acceleration voltage was 40 kV. The 2θ of scanning samples ranged from 3 to 40° at the speed was 0.5 s/step and an angular increment of 0.02°.

The surface morphology and particle size distribution of the Rg3-PLs in the solid state was assessed using a Field Emission Scanning Electron Microscope (FE-SEM; Sigma, Carl Zeiss, UK). The powder was fixed to a carbon-taped stub and coated with a 15 μm thickness of platinum using a sputter coater under vacuum. FE-SEM images were captured at an accelerating voltage of 10 kV. The size distribution histogram of the Rg3-PLs was obtained and plotted using a particle size analyzer (Mastersizer 3000, Malvern Panalytical, UK) equipped with an Aero unit, where dry powder was dispersed in the air.

2.3.2. Characterization of liposomes reconstituted from Rg3-PLs

The generation of liposomal dispersion from Rg3-PLs powder was made by simply dispersing 10 mg of blank PLs or Rg3-PLs in 1 mL of DDW and shaking for 5 min. An electrophoretic DLS size analyzer (ELS-Z, Otsuka Electronics, Japan) was used to observe the average of size, particle distribution, polydispersity index (PI) of the reconstituted liposomes. The zeta potential of liposomal dispersion was separately measured in PBS pH 7.4.

The entrapment efficiency (EE) of Rg3 in the reconstituted liposomes was determined by following protocol: The undissolved Rg3 was removed from the liposomal dispersion by filtering through a 0.45 μm cellulose acetate membrane (Minisart RC15, Sartorius, Germany). Then, 100 μL of the filtrate aliquot was added to acetonitrile (900 μL), and then vortex-mixed for 30 min to disrupt the liposomal structure. The concentration of Rg3 in the sample was determined by the LC−MS/MS method described above. The EE of Rg3 in the reconstituted Rg3-PLs liposomes (%) was calculated by the following equation:

$$\text{Entrapment efficiency of Rg3 } (\%) = \frac{E}{E_0} \times 100$$

where E_0 is the initial Rg3 amount added to prepare the Rg3-PLs (mg) and E is the amount of Rg3 measured by LC−MS/MS analysis (mg).

For the observation of transmission electron microscopy (TEM) images, one drop of reconstituted liposomal dispersion of Rg3-PLs was placed onto the surface of a copper grid pre-coated with 200-mesh carbon (Electron Microscopy Sciences, USA). Then, uranyl acetate solution was applied to negatively stain the liposomal particles. The samples were dried at room temperature after the removal of the excessive liquid by filter paper. The TEM image was observed using JEM1010 (JEOL, Tokyo, Japan) at an accelerating voltage of 80 kV.

2.4. In vitro release of Rg3

The dialysis membrane method was applied for the *in vitro* release study of Rg3 from the Rg3-PLs, as previously reported with minor modification [23]. Briefly, after dispersing an aliquot (100 μ g as Rg3) of Rg3-PLs powder or Rg3 extract in DDW (3 mL), it was put into a dialysis bag (MWCO 12–14 kDa) and sealed. Then, the bag was immersed into a

conical tube containing 27 mL of release media. To maintain the sink condition, the release media was phosphate buffer (pH 6.8) supplemented with 0.5% (w/v) of SDS, based on aqueous solubility of Rg3 (Table S1, Supplementary Information). These tubes were placed in a water bath at 37 °C and shaken horizontally at a speed of 50 rpm. An aliquot (0.5 mL) of release media was collected at predetermined time points (0.25, 0.5, 1, 2, 4, 6, 8, 12 and 24 h) and an equal volume of media was refilled. The samples appropriately diluted with methanol, and then the concentration of Rg3 was analyzed by the LC–MS/MS method as described above. The cumulative release profile of Rg3 (F; %) against time (t) was plotted and fitted to the following mathematical models:

$$\text{First} - \text{order model} : F = F_{max} \times \left(1 - e^{-kt}\right) \quad (1)$$

$$\text{Higuchi model} : F = k_H \times t^{0.5} \quad (2)$$

$$\text{Korsmeyer–Peppas model} : F = k_{KP} \times t^n \quad (3)$$

$$\text{Hixson} - \text{Crowell model} : F = 100 \times \left[1 - (1 - k_{HC} \times t)^3\right] \quad (4)$$

where k, k_H, k_{KP} and k_{HC} represent the release rate constants of each model, whereas F_{max} is the maximum cumulative amount of Rg3 released. The data were analyzed using an add-in DDSolver program in Microsoft Excel [23–26].

2.5. In vivo pharmacokinetic study

The *in vivo* pharmacokinetics of Rg3 were investigated after oral administration of Rg3-PLs or Rg3 extract in male Sprague–Dawley rats at a dose of 5 mg/kg Rg3. The rats weighing 300 ± 5 g were obtained from Hanlim (Sungnam, South Korea) and were housed in the Animal Center for Pharmaceutical Research, College of Pharmacy, Seoul National University (Seoul, Korea) a light-controlled room (12 h of light and 12 h of dark cycles) at 22 ± 2 °C and a relative humidity of 55 ± 5%. The protocol for the animal studies was approved by the Animal Care and Use Committee of Seoul National University (IRB No SNU-190527-2). Under anesthesia by intramuscular injection of Zoletil® 50 at 50 mg/kg, Intramedic™ polyethylene tubing (PE-50; Becton Dickinson Diagnotics, Sparks Glencoe, MD, USA) was cannulated at the femoral artery of each rat. Rg3 extraction or Rg3-PLs was suspended in DDW (2 mL) and immediately administered orally using an oral zonde needle at a dose of 5 mg/kg as Rg3. Then, blood samples (approximately 150 μL) were collected from the femoral artery at predetermined time intervals (5, 15, 30, 60, 90, 120, 240, 360, 480 min), and the same volume of normal saline (0.9% sodium chloride solution) containing heparin (20 IU/mL) was replenished. After centrifugation of blood samples at 16,000×g for 3 min at 4 °C, plasma supernatants were collected and were kept at −20 °C. The protein in each plasma sample (50 μL) was precipitated by adding 250 μL of acetonitrile containing valsartan (100 ng/mL). They were vortexed for 15 min before being centrifuged at 16,000×g for 5 min. Then, 5 μL of each supernatant was injected into the LC–MS/MS system, as described above. Following noncompartmental pharmacokinetic parameters were calculated by the WinNonlin® (Version 3.1, Pharsight, Mountain View, CA, USA): peak plasma concentration (C_{max}), time to reach C_{max} (T_{max}) and total area under the plasma concentration-time curve from zero to 480 min (AUC_t). Relative bioavailability was calculated by (Eq. (5)).

$$\text{Relative bioavailability}\ (\%) = 100 \times \frac{AUC_t^{Rg3-PLs} \times D_{Rg3\ extract}}{AUC_t^{Rg3\ extract} \times D_{Rg3-PLs}} \quad (5)$$

where:

$AUC_t^{Rg3-PLs}$, $AUC_t^{Rg3\ extract}$: AUC_t of Rg3-PLs and Rg3 extract groups, respectively

$D_{Rg3-PLs}$, $D_{Rg3\ extract}$: Dose of Rg3 in formulation administrated in rats (5 mg/kg)

2.6. In vitro cytotoxicity study

The cytotoxicity of Rg3 extract, blank PLs and Rg3-PLs was evaluated by an *in vitro* viability assay in human colorectal adenocarcinoma (Caco-2) cells (Korean Cell Line Bank, Seoul, South Korea) [27,28]. Briefly, Caco-2 cells were cultured in DMEM supplemented with 10% (*v/v*) FBS and 0.5% (*v/v*) penicillin–streptomycin in an incubator at 37 °C with 5% CO_2 atmosphere and 95% relative humidity. In each well of 96-well plates, 1×10^4 cells/well were seeded and grown for 24 h prior to the experiments. Each well was treated with either Rg3 extract, blank PLs or Rg3-PLs at concentrations ranging from 2 to 2000 μg/mL, followed by incubation for 24 h or 48 h. Then, the 3-(4,5-dimethylthiazol-2-yl)-5 (3-carboxymethoxyphenyl)-2-(4-sulfophenyl)-2H-tetrazolium (MTS) reagent (CellTiter 96 Aqueous One Solution Cell Proliferation Assay, Promega, Milan, Italy) dissolved in complete media was applied according to the manufacturer's instructions. Followed by an additional incubation for 4 h at 37 °C, the absorbance of the plates was read at 492 nm using a microplate reader (Multiskan Microplate Spectrophotometer; Thermo Fisher Scientific, MA, USA).

2.7. Statistical analysis

All experiments were performed at least three times independently, and the acquired results are presented as the mean ± standard deviation (S.D.). Student's t-test was performed for statistical analysis (GraphPad Prism ver. 9.5.0, San Diego, CA, USA). A p *value* < 0.05 was considered significantly different.

3. Results and discussion

3.1. Preparation and physicochemical characterization of Rg3-PLs

The solvent evaporation-on-matrix method was applied to prepare the Rg3-PLS following the method previously reported with slight modification [13,16]. Ethanol and DDW mixtures were evaporated using a rotary evaporator, followed by the removal of the remaining DDW by lyophilization (Fig. 1A). This stepwise removal process could prevent the melting of the lyophilizate by the remaining ethanol, which in turn could enhance the homogeneity of the lyophilized product. Moreover, since the Rg3 extract contains unknown excipient(s) that are insoluble in ethanol, it was slowly added into the ethanol/DDW mixture to prevent precipitation. No visible precipitation was observed during the rotary evaporation process, and the lyophilizate did not melt during the lyophilization process, indicating complete evaporation of ethanol and compromising the homogeneity of the Rg3-PLs powder. As shown in Fig. 1A, pale yellowish Rg3-PLs powder with 0.2% Rg3 content was obtained after grinding and sieving (Table 1). These results were consistent with the characterization of the Pg3-PLs powder by FE-SEM

Table 1
Physicochemical characterization of blank PLs and Rg3-PLs.

State of proliposomes	Parameter	Blank PLs	Rg3-PLs
Solid powder	Rg3 content (%, w/w)	–	0.2 ± 0.0
Reconstituted liposomal suspension	Particle size (nm)	365.6 ± 14.5	352.1 ± 11.1
	Polydispersity index (PDI)	0.28 ± 0.02	0.30 ± 0.03
	Zeta potential (mV)	−31.4 ± 0.4	−28.6 ± 0.1
	Entrapment efficiency of Rg3 (%)	–	97.3 ± 1.5
	Rg3 loading content (%, w/v)		0.19 ± 0.01

Data represent the mean ± S.D. (n = 3).

images (Fig. 1B) and DLS analyzer (Fig. 1C).

The X-ray diffractograms of the Rg3-PLs and its excipients, including the physical mixture, are shown in Fig. 1D. Both Rg3 and Rg3 extract diffractograms exhibited sharp peaks at approximately 6.4 and 8.5°, which indicates that Rg3 exists as a crystalline form [29]. The physical mixture also showed characteristic crystalline diffraction peaks of Rg3. On the other hand, distinctive crystalline diffraction peaks of Rg3 disappeared in Rg3-PLs, showing broad peaks similar to those of blank PLs. The disappearance of the crystalline peaks of Rg3 in Rg3-PLs implies that Rg3 was incorporated in an amorphous form during the preparation process, which is consistent with previous reports [13,30,31]. The amorphous form of Rg3 in Rg-PLs would be critical in terms of improving the solubility and dissolution of Rg3 in the gastrointestinal tract, thereby enhancing its oral bioavailability [32].

3.2. Characterization of liposomes reconstituted from Rg3-PLs

Table 1 summarizes the mean particle size and zeta potential of liposomes generated after reconstitution of the blank PLs or Rg3-PLs powder in DDW by gentle hand-shaking for 5 min. Nanosized liposomal dispersions were obtained with mean diameters of approximately 365 and 352 nm from the blank PLs and Rg3-PLs, respectively, and they were not significantly different. The particle size distribution (Fig. 2A) and TEM images (Fig. 2B) of the dispersions were consistent with the results of the dynamic light scattering (DLS) analysis. Although the presence of micron-sized liposomes was observed in the size distribution in Fig. 2B, the PDI values of the blank PLs and Rg-PLs were approximately 0.3, supporting the particle size homogeneity of liposomal dispersions. Moreover, TEM images confirmed that the liposomal particles generated from the reconstitution of the blank PLs and Rg3-PLs powder were in the form of a characteristic small unilamellar vesicle structure with a typical PC bilayer (Fig. 2B). The surface charge of both liposomal particles showed a negative charge of approximately −30 mV (Table 1), which is similar to that of the PC liposomal formulation previously reported [33,34]. This anionic surface charge was reported to promote the oral absorption of liposomes *via* clathrin-dependent endocytosis and micropinocytosis pathway in intestinal epithelial cells [35]. These results imply the high physical stability of the liposomes after reconstitution and that entrapment of Rg3 did not affect the characteristics of PLs, including the particle size and zeta potential [13]. It is notable that the EE of Rg3 in the reconstituted liposomes was relatively high (97.32%) (Table 1), indicating that gentle hand-shaking for 5 min was enough to successfully convert Rg3-PLs powder to form a liposomal dispersion with a high EE of Rg3. Thus, it is plausible that orally administered Rg3-PLs powder would experience a similar conversion process by movement of the gastrointestinal tract. Moreover, the particles size of the dispersed liposome maintained less than 400 nm for at least 24 h, implying their physicochemical stability (Supplementary Information Fig. S1).

3.3. In vitro release of Rg3

The *in vitro* release profiles of Rg3 from Rg3-PLs and Rg3 extract are shown in Fig. 3A, which was conducted at pH 6.8 for 24 h by the dialysis membrane method in sink conditions. The cumulative amount of Rg3 released for 24 h from the Rg3 extract was less than 5% due to its poor aqueous solubility (approximately 3.2 μg/mL) [3,4,36]. However, the release amount of Rg3 from Rg3-PLs was significantly enhanced

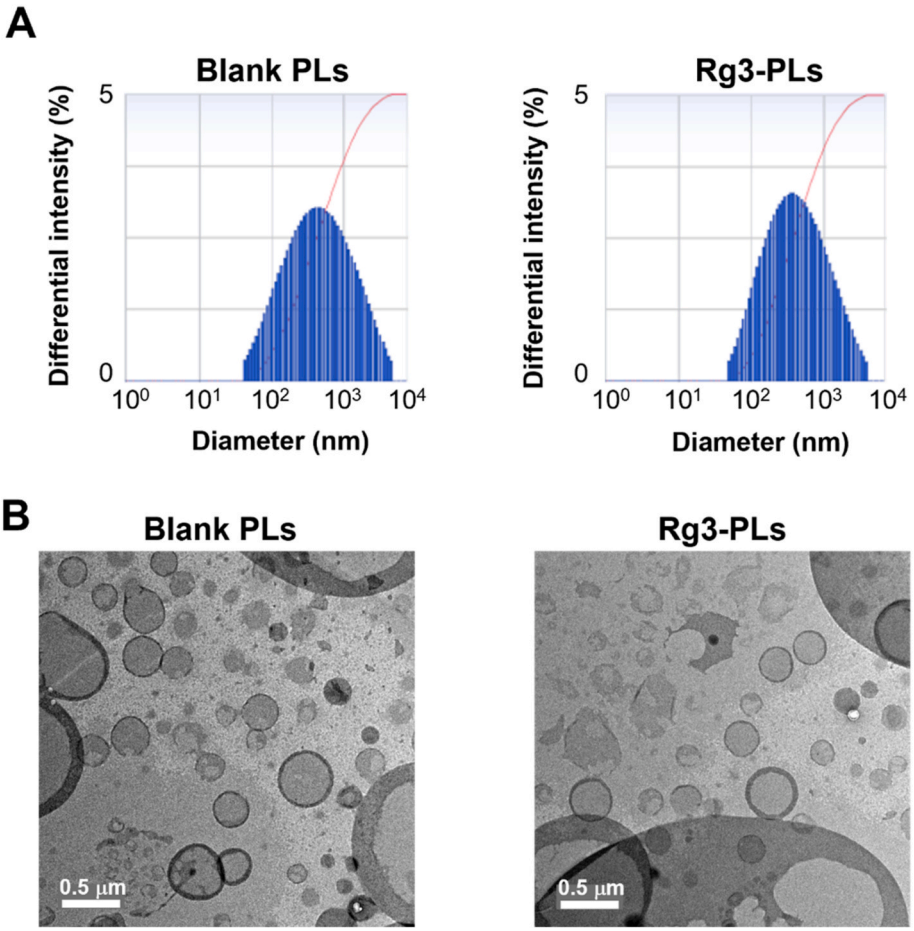

Fig. 2. (A) Particle size distribution and (B) TEM images of the blank PLs and Rg3-PLs after reconstitution. The length of the scale bar is 0.5 μm.

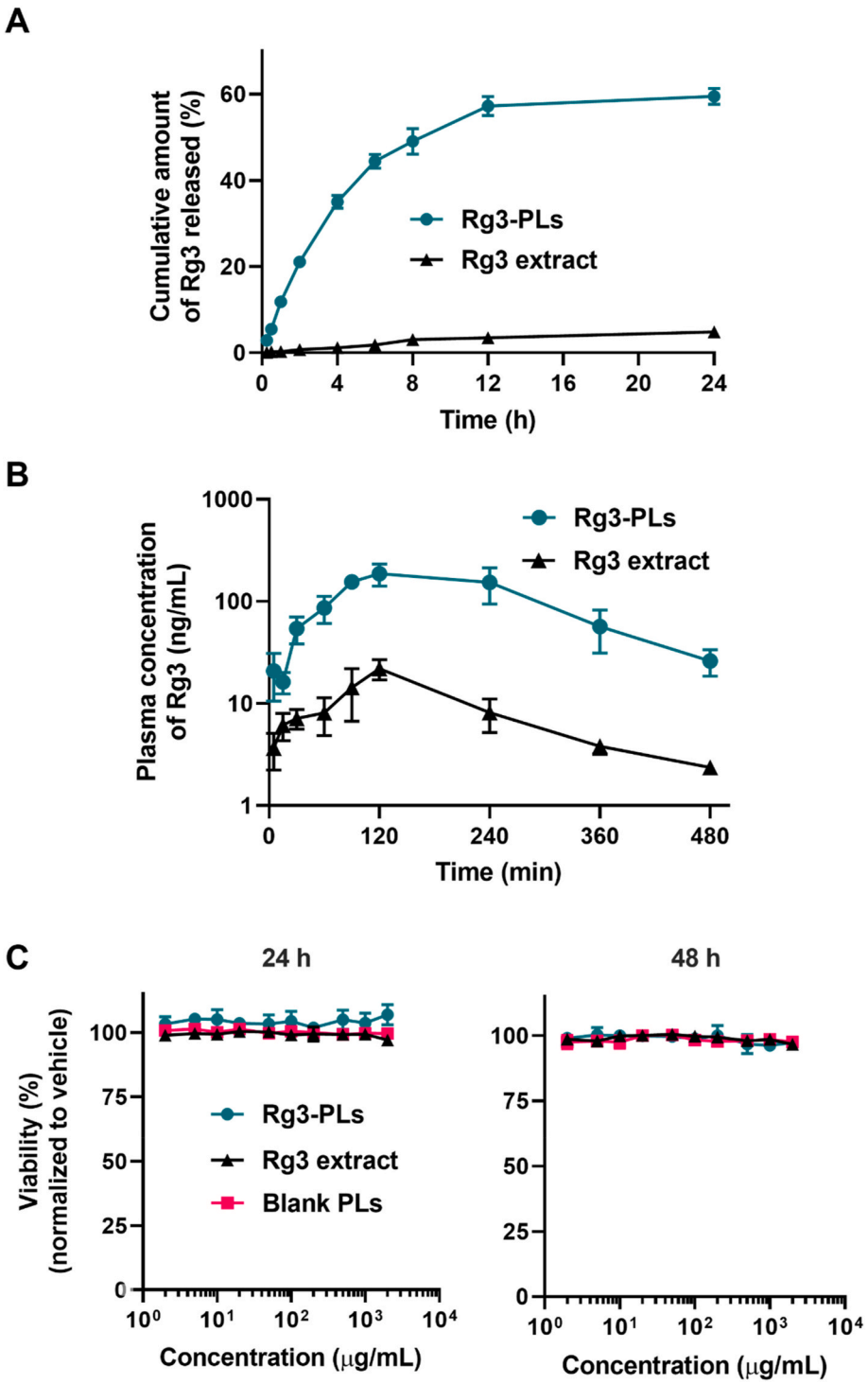

Fig. 3. (A) *In vitro* release profiles of Rg3 from Rg3-PLs and Rg3 extract (mean ± S.D., n = 3) and (B) Plasma concentration profiles of Rg3 after oral administration of Rg3-PLs or Rg3 extract at a dose of 5 mg/kg as Rg3 in rats (mean ± S.D., n = 4). (C) *In vitro* cytotoxicity of Rg3 extract, blank PLs and Rg3-PLs on Caco-2 cells (mean ± S.D., n = 3).

compared with that from the Rg3 extract group, reaching up to 60% during the same period. Then, the *in vitro* release profiles of Rg3 from Rg3-PLs were fitted to various mathematical release kinetic models to understand the release mechanism(s) of Rg3. The highest coefficient of determination ($R^2 = 0.9976$) was observed with the first-order kinetic model (Table 2). This indicated that the release of Rg3 could be highly dependent on the Rg3 amount in the Rg3-PLs formulation [37]. Thus, high entrapment of Rg3 into the reconstituted liposomes (up to 97.3%, Table 1) could have contributed to its enhanced dissolution. In addition, the amorphous state of Rg3 in the Rg3-PLs powder (Fig. 1B) could also have enhanced its dissolution and/or rapid entrapment into the liposomes, while crystalline Rg3 in the Rg3 extract resulted in a slow and poor release profile. Moreover, it is noteworthy that rapid and successful conversion of Rg3-PLs into Rg3-loaded liposomes was achieved at low shear stress in a gentle shaking water bath at 50 rpm. Thus, it is expected that oral administration of Rg3-PLs would enhance the dissolution of Rg3 by rapid conversion into liposomes in the gastrointestinal tract, which in turn leads to an increase in the oral bioavailability of Rg3.

Table 2
Kinetic models of the *in vitro* release of Rg3 from the Rg3-PLs.

Model	Equation	Constant	R^2
First order	$F = F_{max} \times (1-e^{-kt})$	$k = 0.216$	0.9976
Higuchi	$F = k_H \times t^{0.5}$	$k_H = 14.79$	0.8951
Korsmeyer-Peppas	$F = k_{KP} \times t^n$	$k_{KP} = 17.23$ $n = 0.436$	0.9079
Hixson-Crowell	$F = 100 \times [1 - (1 - k_{HC} \times t)^3]$	$k_{HC} = 0.02$	0.6869

The goodness of fit is presented as R^2. F_{max} is the maximum cumulative amount released, whereas k, k_H, k_{KP} and k_{HC} are the release rate constants of each model.

3.4. *In vivo* pharmacokinetic study

The plasma concentration of Rg3 *versus* time profiles are plotted in Fig. 3B, where Rg3 extract or Rg3-PLs formulations were orally administered in rats at a dose of 5 mg/kg as Rg3. Their pharmacokinetic parameters calculated by using noncompartmental analysis are summarized in Table 3. The average C_{max} value of the Rg3-PLs group was 8.8-fold higher compared with that of the Rg3 extract group ($p < 0.0001$), which could be due to the enhanced dissolution of Rg3 in the gastrointestinal fluid. The systemic exposure of Rg3 also significantly increased in the Rg3-PLs group, resulting in 11.8-fold higher AUC_t and relative bioavailability values compared to those of the Rg3 extract group. These *in vivo* results were consistent with the enhanced *in vitro* dissolution of Rg3 from Rg3-PLs (Fig. 3A). Because of the poor solubility of Rg3 in water, the dissolution of Rg3 in the gastrointestinal tract could be the rate-limiting step for its oral absorption [3,4]. Thus, the improvement in dissolution by forming Rg3-loaded liposomes after oral administration of Rg3-PLs could be attributed to the enhanced absorption of Rg3, leading to an increase in bioavailability. Moreover, the T_{max} values of the Rg3 extract and Rg3-PLs groups were not significantly different, implying that the dissolution and absorption processes of the two groups are comparably immediate and rapid. The terminal phase half-life ($T_{1/2}$) of Rg3 in plasma calculated from both the Rg3 extract group and Rg3-PLs group was approximately 2–2.5 h, which was consistent with previous results (2.3–4.4 h) [38–41].

Previous pharmacokinetic studies reported very poor oral absorption and low absolute bioavailability (<20%) of ginsenosides, claiming that the hydrolysis triggered by the gut microbiota could be a reason [40,42–44]. On the other hand, the Rg3-PLs formulation could be advantageous because the encapsulation of hydrophobic ginsenosides (including Rg3) into the phospholipid bilayer of liposomes could protect them from preabsorption metabolism, which would eventually contribute to enhancing their oral bioavailability. Moreover, the lymphatic absorption pathway of liposomes could also have partially contributed to the enhancement of oral bioavailability of Rg3 by bypassing hepatic first-pass metabolism [45]. Thus, these advantages of liposomal formulation could have additively resulted in significant enhancement of oral bioavailability of Rg3, among which rapid dissolution and absorption of amorphous Rg3 in the Rg3-PLs formulation could be one major mechanism.

3.5. *In vitro* cytotoxicity study

Fig. 3C shows the *in vitro* viability of Caco-2 cells evaluated by using the MTS-based assay after applying various concentrations of Rg3 extract, blank PLs or Rg3-PLs for 24 h or 48 h. The average cell viability of all groups was higher than 95% of the untreated control within the tested concentration ranges (2–2000 μg/mL). These results demonstrated their biocompatibility at the cellular level, and are consistent with those of previous studies reporting a low toxicity of Rg3 in mice, rats and humans [46]. Moreover, the pharmaceutical excipients for the preparation of Rg3-PL3, including SPC and sorbitol, are reported to be nontoxic, and thus, this vehicle is unlikely to be associated with any gastrointestinal toxicity after oral administration [13].

Table 3
Pharmacokinetic parameters of Rg3 after oral administration of Rg3 extract or Rg3-PLs at a dose of 5 mg/kg as Rg3 in rats.

Parameters	Rg3 extract	Rg3-PLs
C_{max} (ng/mL)	21.89 ± 4.87	192.00 ± 40.11****
T_{max} (min)	120.0 ± 0.0	105.3 ± 17.3$^{n.s.}$
$T_{1/2}$ (min)	164.7 ± 83.0	115.4 ± 26.9$^{n.s.}$
AUC_t (μ g × min/mL)	4.2 ± 0.7	49.6 ± 6.9****
Relative bioavailability (%)	100	1181

Data represent the mean ± S.D. (n = 4).
****$p < 0.0001$ compared to the Rg3 extract group.
$^{n.s.}$ not significantly different compared to the Rg3 extract group.

4. Conclusion

Diverse liposomal formulations have been reported to improve the oral bioavailability of poorly water-soluble ginsenosides, yet the physical instability of liposomes has been a major inherent obstacle for their clinical application. We investigated the Rg3-PLs formulation as an alternative to liposomes for oral administration of ginsenosides using ginsenoside Rg3 (Rg3) as a marker. PXRD supports that Rg3 was incorporated into PLs in an amorphous form. Solid Rg3-PLs powder rapidly converted to a liposomal dispersion by gentle hand-shaking in water and enhanced the *in vitro* release of Rg3. Moreover, the relative oral bioavailability of Rg3-PLs increased approximately 11.8-fold in compared with that of the Rg3 extract in rats. Rapid dissolution and absorption of amorphous Rg3 in the Rg3-PLs formulation could be a major mechanism of enhancement. Thus, PLs formulation could be a promising strategy for enhancing the oral bioavailability of ginsenosides with storage stability and needs further translational research for clinical application.

Declaration of competing interest

The authors declare that they have no competing financial interests or personal relationships that could have influenced the work reported in this paper.

Acknowledgments

This work was supported by the research grant of the Korean Society of Ginseng (2017) and the National Research Foundation of Korea (NRF) grant funded by the Ministry of Science and ICT (No. NRF-2018R1A5A2024425 and NRF-2020R1A2C2099983).

Appendix A. Supplementary data

Supplementary data to this article can be found online at https://doi.org/10.1016/j.jgr.2024.03.004.

References

[1] Yu SE, Mwesige B, Yi YS, Yoo BC. Ginsenosides: the need to move forward from bench to clinical trials. J Ginseng Res 2019;43:361–7. https://doi.org/10.1016/j.jgr.2018.09.001.
[2] Xiang YZ, Shang HC, Gao XM, Zhang BL. A comparison of the ancient use of ginseng in traditional Chinese medicine with modern pharmacological experiments and clinical trials. Phytother Res 2008;22:851–8. https://doi.org/10.1002/ptr.2384.
[3] Kim H, Lee JH, Kim JE, Kim YS, Ryu CH, Lee HJ, et al. Micro-/nano-sized delivery systems of ginsenosides for improved systemic bioavailability. J Ginseng Res 2018;42:361–9. https://doi.org/10.1016/j.jgr.2017.12.003.
[4] Tawab MA, Bahr U, Karas M, Wurglics M, Schubert-Zsilavecz M. Degradation of ginsenosides in humans after oral administration. Drug Metabol Dispos 2003;31:1065–71. https://doi.org/10.1124/dmd.31.8.1065.
[5] Nekkanti V, Wang Z, Betageri GV. Pharmacokinetic evaluation of improved oral bioavailability of valsartan: proliposomes versus self-nanoemulsifying drug delivery system. AAPS PharmSciTech 2016;17:851–62. https://doi.org/10.1208/s12249-015-0388-8.

[6] Voruganti S, Qin JJ, Sarkar S, Nag S, Walbi IA, Wang S, et al. Oral nano-delivery of anticancer ginsenoside 25-OCH3-PPD, a natural inhibitor of the MDM2 oncogene: nanoparticle preparation, characterization, in vitro and in vivo anti-prostate cancer activity, and mechanisms of action. Oncotarget 2015;6:21379–94. https://doi.org/10.18632/oncotarget.4091.
[7] Jin X, Zhang ZH, Sun E, Tan X Bin, Li SL, Cheng XD, et al. Enhanced oral absorption of 20(S)-protopanaxadiol by self-assembled liquid crystalline nanoparticles containing piperine: in vitro and in vivo studies. Int J Nanomed 2013;8:641–52. https://doi.org/10.2147/IJN.S38203.
[8] Hong C, Wang D, Liang J, Guo Y, Zhu Y, Xia J, et al. Novel ginsenoside-based multifunctional liposomal delivery system for combination therapy of gastric cancer. Theranostics 2019;9:4437–49. https://doi.org/10.7150/thno.34953.
[9] Tran P, Park JS. Recent trends of self-emulsifying drug delivery system for enhancing the oral bioavailability of poorly water-soluble drugs. Journal of Pharmaceutical Investigation 2021;51(4):439–63. https://doi.org/10.1007/S40005-021-00516-0. 2021;51.
[10] Son GH, Lee BJ, Cho CW. Mechanisms of drug release from advanced drug formulations such as polymeric-based drug-delivery systems and lipid nanoparticles. J Pharm Investig 2017;47:287–96. https://doi.org/10.1007/s40005-017-0320-1.
[11] Noh G, Keum T, Bashyal S, Seo JE, Shrawani L, Kim JH, et al. Recent progress in hydrophobic ion-pairing and lipid-based drug delivery systems for enhanced oral delivery of biopharmaceuticals. J Pharm Investig 2022;52:75–93. https://doi.org/10.1007/s40005-021-00549-5.
[12] Kim JS. Liposomal drug delivery system. J Pharm Investig 2016;46:387–92. https://doi.org/10.1007/s40005-016-0260-1.
[13] Jeon D, Kim K-T, Baek M-J, Kim DH, Lee J-Y, Kim D-D. Preparation and evaluation of celecoxib-loaded proliposomes with high lipid content. Eur J Pharm Biopharm 2019;141:139–48. https://doi.org/10.1016/j.ejpb.2019.05.025.
[14] Kim MH, Kim DH, Nguyen DT, Lee HS, Kang NW, Baek MJ, et al. Preparation and evaluation of Eudragit l100-PEG proliponiosomes for enhanced oral delivery of celecoxib. Pharmaceutics 2020;12:1–14. https://doi.org/10.3390/pharmaceutics12080718.
[15] Adel IM, Elmeligy MF, Abdelrahim MEAE, Maged A, Abdelkhalek AA, Abdelmoteleb AMMM, et al. Design and characterization of spray-dried proliposomes for the pulmonary delivery of curcumin. Int J Nanomed 2021;16:2667–87. https://doi.org/10.2147/IJN.S306831.
[16] Jahn A, Song CK, Balakrishnan P, Hong SS, Lee JH, Chung SJ, et al. AAPE proliposomes for topical atopic dermatitis treatment. J Microencapsul 2014;31:768–73. https://doi.org/10.3109/02652048.2014.932027.
[17] Karn PR, Jin SE, Lee BJ, Sun BK, Kim MS, Sung JH, et al. Preparation and evaluation of cyclosporine A-containing proliposomes: a comparison of the supercritical antisolvent process with the conventional film method. Int J Nanomed 2014;9:5079–91. https://doi.org/10.2147/IJN.S70340.
[18] Byeon JC, Lee SE, Kim TH, Ahn J bin, Kim DH, Choi JS, et al. Design of novel proliposome formulation for antioxidant peptide, glutathione with enhanced oral bioavailability and stability. Drug Deliv 2019;26:216–25. https://doi.org/10.1080/10717544.2018.1551441.
[19] Arregui JR, Kovvasu SP, Betageri GV. Daptomycin proliposomes for oral delivery: formulation, characterization, and in vivo pharmacokinetics. AAPS PharmSciTech 2018;19:1802–9. https://doi.org/10.1208/s12249-018-0989-0.
[20] Sharma S, Jyoti K, Sinha R, Katyal A, Jain UK, Madan J. Protamine coated proliposomes of recombinant human insulin encased in Eudragit S100 coated capsule offered improved peptide delivery and permeation across Caco-2 cells. Mater Sci Eng C 2016;67:378–85. https://doi.org/10.1016/j.msec.2016.05.010.
[21] Kim MH, Kim DH, Nguyen DT, Lee HS, Kang NW, Baek MJ, et al. Preparation and evaluation of Eudragit l100-PEG proliponiosomes for enhanced oral delivery of celecoxib. Pharmaceutics 2020;12:1–14. https://doi.org/10.3390/pharmaceutics12080718.
[22] Bankole VO, Osungunna MO, Souza CRF, Salvador SL, Oliveira WP. Spray-dried proliposomes: an innovative method for encapsulation of Rosmarinus officinalis L. Polyphenols. AAPS PharmSciTech 2020;21:143. https://doi.org/10.1208/s12249-020-01668-2.
[23] Baek MJ, Shin HJ, Park JH, Kim J, Kang IM, Lee JI, et al. Preparation and evaluation of the doxazosin-bentonite composite as a pH-dependent controlled-release oral formulation. Appl Clay Sci 2022;229:106677. https://doi.org/10.1016/J.CLAY.2022.106677.
[24] Zhang Y, Huo M, Zhou J, Zou A, Li W, Yao C, et al. DDSolver: an add-in program for modeling and comparison of drug dissolution profiles. AAPS J 2010;12:263–71. https://doi.org/10.1208/s12248-010-9185-1.
[25] Nguyen DT, Kim MH, Yu NY, Baek MJ, Kang KS, Lee KW, et al. Combined orobol-bentonite composite formulation for effective topical skin targeted therapy in mouse model. Int J Nanomed 2022;17:6513. https://doi.org/10.2147/IJN.S390993.
[26] Baek MJ, Park JH, Nguyen DT, Kim D, Kim J, Kang IM, et al. Bentonite as a water-insoluble amorphous solid dispersion matrix for enhancing oral bioavailability of poorly water-soluble drugs. J Contr Release 2023;363:525–35. https://doi.org/10.1016/J.JCONREL.2023.09.051.
[27] Kang NW, Lee JY, Kim DD. Hydroxyapatite-binding albumin nanoclusters for enhancing bone tumor chemotherapy. J Contr Release 2022;342:111–21. https://doi.org/10.1016/j.jconrel.2021.12.039.
[28] Lee HS, Kang NW, Kim H, Kim DH, Chae J woo, Lee W, et al. Chondroitin sulfate-hybridized zein nanoparticles for tumor-targeted delivery of docetaxel. Carbohydr Polym 2021;253:117187. https://doi.org/10.1016/J.CARBPOL.2020.117187.
[29] Blandizzi C, Viscomi GC, Scarpignato C. Impact of crystal polymorphism on the systemic bioavailability of rifaximin, an antibiotic acting locally in the gastrointestinal tract, in healthy volunteers. Drug Des Dev Ther 2014;9:1–11. https://doi.org/10.2147/DDDT.S72572.
[30] Salonen J, Laitinen L, Kaukonen AM, Tuura J, Björkqvist M, Heikkilä T, et al. Mesoporous silicon microparticles for oral drug delivery: loading and release of five model drugs. J Contr Release 2005;108:362–74. https://doi.org/10.1016/j.jconrel.2005.08.017.
[31] Kapoor S, Hegde R, Bhattacharyya AJ. Influence of surface chemistry of mesoporous alumina with wide pore distribution on controlled drug release. J Contr Release 2009;140:34–9. https://doi.org/10.1016/j.jconrel.2009.07.015.
[32] Tang C, Wang Y, Long Y, An X, Shen J, Ni Y. Anchoring 20(R)-Ginsenoside Rg3 onto cellulose nanocrystals to increase the hydroxyl radical scavenging activity. ACS Sustainable Chem Eng 2017;5:7507–13. https://doi.org/10.1021/acssuschemeng.6b02996.
[33] Serrano G, Almudéver P, Serrano JM, Milara J, Torrens A, Expósito I, et al. Phosphatidylcholine liposomes as carriers to improve topical ascorbic acid treatment of skin disorders. Clin Cosmet Invest Dermatol 2015;8:591–9. https://doi.org/10.2147/CCID.S90781.
[34] Zhang H, Wang T, He W, Wang J, Li X. Irinotecan-loaded ROS-responsive liposomes containing thioether phosphatidylcholine for improving anticancer activity. J Drug Deliv Sci Technol 2022;71:103321. https://doi.org/10.1016/j.jddst.2022.103321.
[35] Du XJ, Wang JL, Iqbal S, Li HJ, Cao ZT, Wang YC, et al. The effect of surface charge on oral absorption of polymeric nanoparticles. Biomater Sci 2018;6. https://doi.org/10.1039/c7bm01096f.
[36] Cui W, Cheng L, Hu C, Li H, Zhang Y, Chang J. Electrospun poly(L-lactide) fiber with ginsenoside Rg3 for inhibiting scar hyperplasia of skin. PLoS One 2013;8:e68771. https://doi.org/10.1371/JOURNAL.PONE.0068771.
[37] Jain A, Jain SK. In vitro release kinetics model fitting of liposomes: an insight. Chem Phys Lipids 2016;201:28–40. https://doi.org/10.1016/j.chemphyslip.2016.10.005.
[38] Jeon JH, Lee J, Choi MK, Song IS. Pharmacokinetics of ginsenosides following repeated oral administration of red ginseng extract significantly differ between species of experimental animals. Arch Pharm Res (Seoul) 2020;43:1335–46. https://doi.org/10.1007/S12272-020-01289-0.
[39] Peng M, Li X, Zhang T, Ding Y, Yi Y, Le J, et al. Stereoselective pharmacokinetic and metabolism studies of 20(S)- and 20(R)-ginsenoside Rg3 epimers in rat plasma by liquid chromatography-electrospray ionization mass spectrometry. J Pharm Biomed Anal 2016;121:215–24. https://doi.org/10.1016/J.JPBA.2016.01.020.
[40] Xie HT, Wang GJ, Sun JG, Tucker I, Zhao XC, Xie YY, et al. High performance liquid chromatographic-mass spectrometric determination of ginsenoside Rg3 and its metabolites in rat plasma using solid-phase extraction for pharmacokinetic studies. J Chromatogr, B: Anal Technol Biomed Life Sci 2005;818:167–73. https://doi.org/10.1016/j.jchromb.2004.12.028.
[41] Fan H, Sun XL, Yaliu S, Lu MM, Xue F, Meng XS, et al. Comparative pharmacokinetics of ginsenoside Rg3 and ginsenoside Rh2 after oral administration of ginsenoside Rg3 in normal and walker 256 tumor-bearing rats. Phcog Mag 2016;12:21. https://doi.org/10.4103/0973-1296.176014.
[42] Won HJ, Kim H Il, Park T, Kim H, Jo K, Jeon H, et al. Non-clinical pharmacokinetic behavior of ginsenosides. J Ginseng Res 2019;43:354–60. https://doi.org/10.1016/j.jgr.2018.06.001.
[43] Gu Y, Wang GJ, Wu XL, Zheng YT, Zhang JW, Ai H, et al. Intestinal absorption mechanisms of ginsenoside Rh2: stereoselectivity and involvement of ABC transporters. Xenobiotica 2010;40:602–12. https://doi.org/10.3109/00498254.2010.500744.
[44] Gulnaz A, Chang JE, Maeng HJ, Shin KH, Lee KR, Chae YJ. A mechanism-based understanding of altered drug pharmacokinetics by gut microbiota. Journal of Pharmaceutical Investigation 2023;53:73–92. https://doi.org/10.1007/s40005-022-00600-z.
[45] Ahn H, Park JH. Liposomal delivery systems for intestinal lymphatic drug transport. Biomater Res 2016;20:1–6. https://doi.org/10.1186/s40824-016-0083-1.
[46] Li C, Wang Z, Li G, Wang Z, Yang J, Li Y, et al. Acute and repeated dose 26-week oral toxicity study of 20(S)-ginsenoside Rg3 in Kunming mice and Sprague–Dawley rats. J Ginseng Res 2020;44:222–8. https://doi.org/10.1016/J.JGR.2018.10.001.